Design study of the geometry of a punching/blanking tool

U.P. Singh

Department of Mechanical and Industrial Engineering, University of Ulster, Jordanstown, UK

A.H. Streppel and H.J.J. Kals

Department of Mechanical Engineering, Twente University, Enschede, Netherlands

Industrial Summary

The cost of tooling in sheet metal industries contributes a considerable part to the overall cost of manufacturing a component. It is therefore imperative to keep down this cost by ensuring that the tool works for a long period in production without interruption. One way of achieving this objective is to reduce the stress on the tool during punching/blanking.

This paper deals with the study of this problem by using the finite-element technique. 3-D finite-element models of various type of punching/blanking tools have been developed, these models enabling the analysis of the effects of variations in tool geometry on the punching/blanking force and on the deformation of the punch, a parameter highly relevant to the assessment of tool performance in terms of the accuracy of the manufactured components. The model caters also for variation in the characteristics of the tool material, in the sense that a highly wear-resistant tool is normally composed of carbide tips around its cutting profile. Computed results by FE models are checked against design standards by American Society of Manufacturing Engineers (SME). Some suggestions are offered as to how the efficiency of a punching/blanking tool can be improved.

1. Introduction

Experience shows that cost of tooling in sheet metal industries contributes a substantial part to the overall cost of manufacturing a component, so that it is essential to keep down this cost by ensuring that the tool works for a long period without interruption. To achieve this objective a production engineer has the following options: (i) to minimize the deflection of a forming machine tool to be employed in the punching/blanking operation; or (ii) to minimize the deflection of the die-set to be employed on the forming machine; or (iii) to reduce the stress on the punching/blanking tool; or (iv) to effect a combination of the foregoing three options. The options in items (i) and (ii) have been

---

Correspondence to: U.P. Singh, Department of Mechanical and Industrial Engineering, University of Ulster, Jordanstown, UK.

dealt with at length in Refs. [1–6], whilst the option in item (iii) has, so far, been dealt with by experimental means only [7,8]. A survey of the literature suggests that no theoretical or precise empirical relationship is available that can aid tool users in the rational selection of tool parameters resulting in minimum distortion of the tool in operation, thereby improving the tool life and enhancing the quality of the product.

To reduce the stress on the tool and thus enable thicker or more resistant stock to be punched on the same press or to permit the use of lower-rated presses, the employment of a punch or die with ground relief on its face is a common practice. It is reported [7,8] that punching/blanking forces vary with various amounts of shear relief on the tool face. However, there is little information available to tool users as to how the amount of shear relief has to be chosen in practice in relation to the punching force required for a given product.

This paper deals with the design analysis of various types of punches with special attention to their cutting profiles, using the finite-element technique. Results obtained by the finite-element analysis of the punches enable the drawing of specific conclusions with regard to the selection of punches in practice for minimum distortion of the punch and reduced stress on the punch.

2. Modelling of the punch

The punch geometry is shown in Fig. 1. In the present analysis the punch fillet provided adjacent to the intersection of diameters D and D_2 is taken into account in order to represent the actual element geometry. Figure 2 displays the nodal representation of the punch point in the finite-element model, whilst Fig. 3 depicts the nodal representation of the different punches considered.
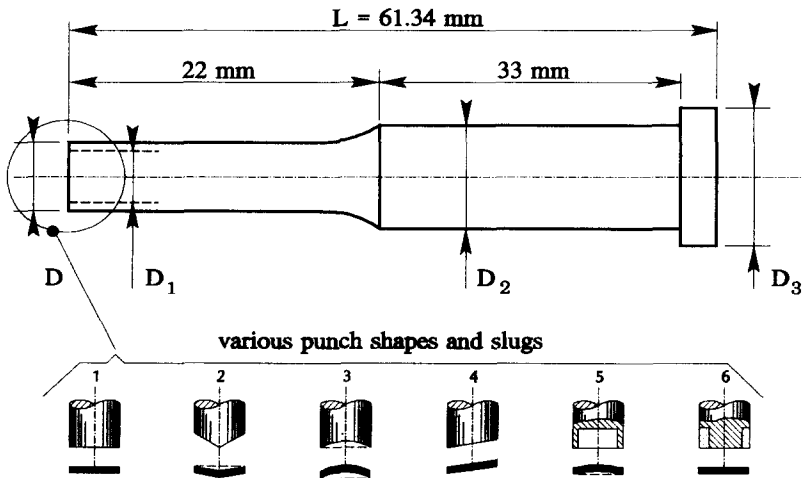

Fig. 1. Punch configuration with various punch shapes and slugs.

The nodal coordinates of the punch points shown in Fig. 2 are presented in Table 1. For every element defined by the coordinates in Table 1 at the O-surface there will be a symmetrically placed element in the second, the third and the fourth quadrant, in such way that

$$x'_o = -x_o = -x_o = x_o$$
$$y'_o = y_o = -y_o = -y_o \tag{1}$$
$$z'_o = z_o = z_o = z_o$$

It is convenient to define a parallel surface called the A-surface that is placed at a distance S from the O-surface along the Z-axis (Figs. 4(a) and 4(b)). The points on this surface are obtained by giving an axial motion to those on the O-surface. The point (X_a, Y_a, Z_a) on the A-surface corresponding to the point on the O-surface will be such that

$$\begin{bmatrix} X_a \\ Y_a \\ Z_a \end{bmatrix} = \begin{bmatrix} X_o & 0 \\ Y_o & 0 \\ Z_o & 1 \end{bmatrix} \begin{bmatrix} 1 \\ S_a \end{bmatrix} \tag{2}$$

Equation 2 is used to generate the nodal-point data for the finite-elements models of the punches.
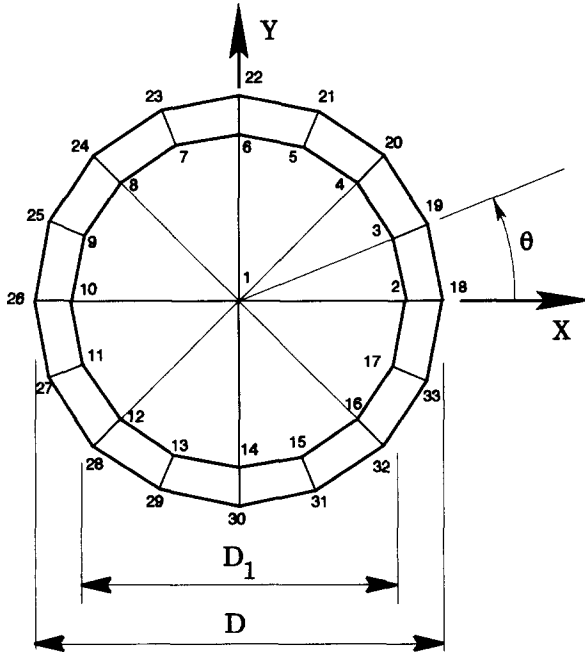

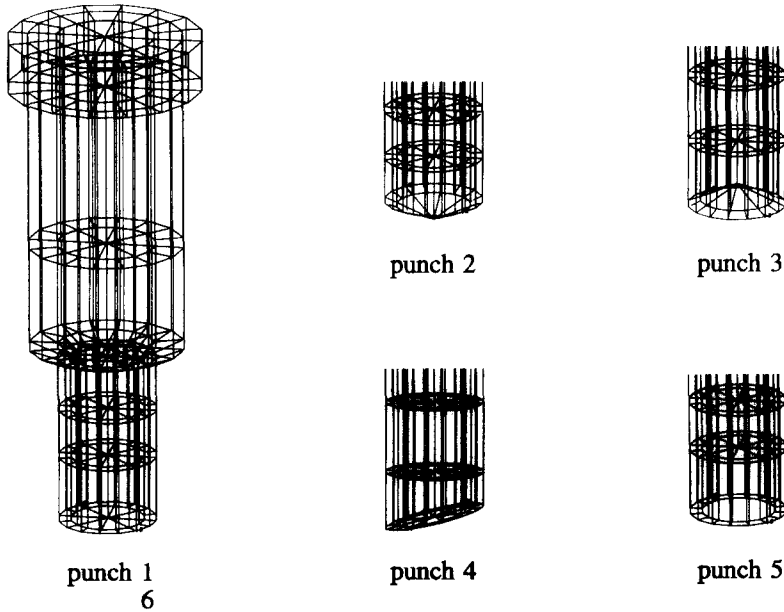Fig. 2. Nodal representation of the geometry of the punch point.

Fig. 3. Finite-element models of the punches: (1) a punch with a flat face; (2) a punch with balanced convex shear; (3) a punch with concave shear; (4) a punch with one-way shear; (5) a punch with an inverted cup-shaped face; and (6) a punch with sintered hard metal around its circumferential cutting edge.

TABLE 1

Coordinates of the punch points on the O-surface

Node No.	θ	Coordinates
1	0	$X_o = 0$, $Y_o = 0$, $Z_o = 0$
2	0	$X_o = D_1/2 \cos \theta$, $Y_o = D_1/2 \sin \theta$, $Z_o = 0$, $Z_o = (D_1/2 \tan \phi)^a$
3	$\pi/8$	$\quad + (D_1/2 \cos \theta \tan \phi)^b$
4	$\pi/4$	
5	$3\pi/8$	
6	$\pi/2$	
18	0	$X_o = D/2 \cos \theta$, $Y_o = D/2 \sin \theta$, $Z_o = 0$, $Z_o = (D/2 \tan \phi)^a$
19	$\pi/8$	$\quad + (D/2 \cos \theta \tan \phi)^b$
20	$\pi/4$	
21	$3\pi/8$	
22	$\pi/2$	

ϕ is the shear angle, as defined in Fig. 9 and θ is defined in Fig. 2.
[a]refers to punches 2 and 3, whilst the second term in the equation is absent.
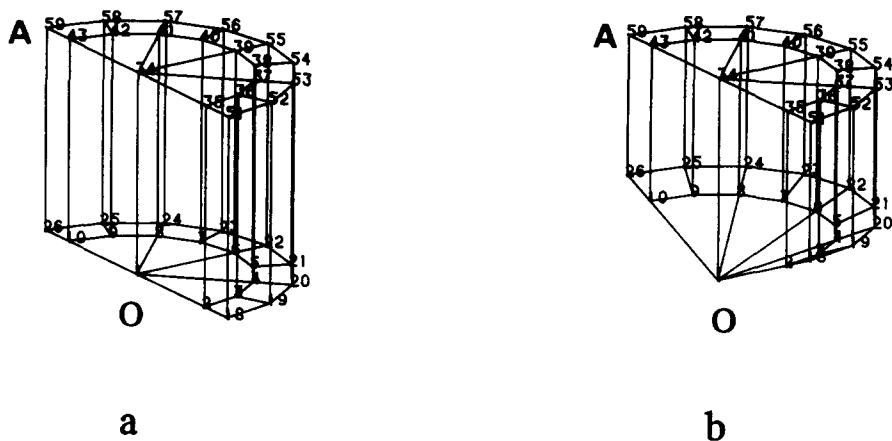[b]refers to punch 4, the first term included.

Fig. 4. Brick configuration and an 8-node element for punch 1,6 (a) and punch 2 (b).

Figure 4 shows the elements of the first quadrant and the corresponding brick forms in the second quadrant. Similar types of elements with their symmetrical counterparts are stacked up to the height of the punch in building the finite-element model for the punch.

The procedure employed to obtain the deformation of the punch is illustrated in Fig. 5, where the material properties, the boundary conditions and the loading conditions need to be supplied as an input to the model. A view of distorted punches 1 and 4 is presented in Fig. 6.

2.1. Boundary condition

The top plate of the die-set containing the punch along with the upper head of the press tends to deflect as the thrust is applied to the punch [6]. Consequently, the top plate of the die-set carrying the punch follows the lateral movements of the top head of the press. To account for these movements, the nodal points on the top surface of the punch should be given a prescribed displacement equivalent to the amount of deflection of the die-set at the punch-head section. As the prime objective of this paper is to analyse the rigidity characteristics of a punch with various design features, it is perfectly justified to set the top surface of the punch fixed. Thus the boundary condition corresponds to simply setting those nodal points on the top surface to zero (see Table 2).

2.2. Punch load

For the analysis of punch deformation, a static load corresponding to the punching load is defined. Young's modulus and Poisson's ratio for the punch material are to be provided. When assuming that the mechanics of punching is based on pure shearing, the instantaneous punching force F_p (see Fig. 7) is as given in Ref. [6]:
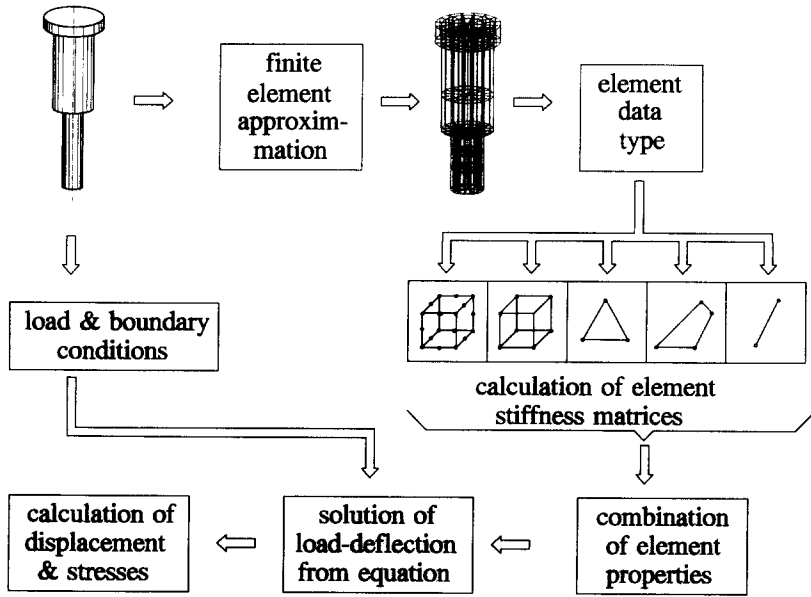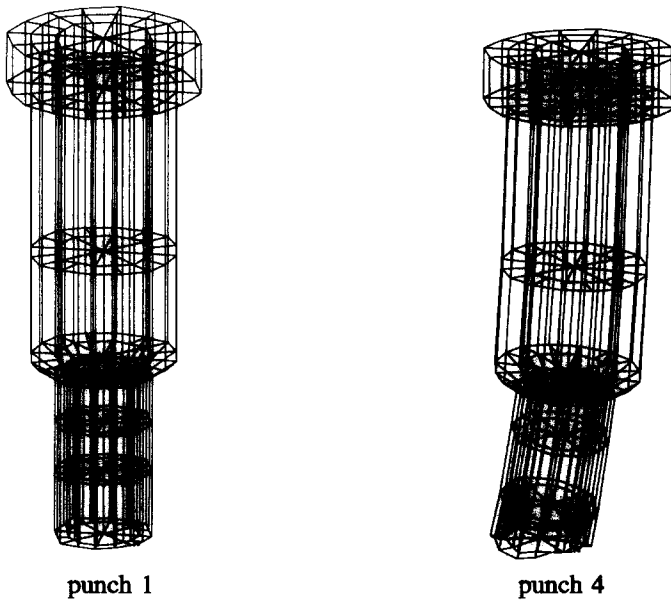
Fig. 5. Finite-element procedure.

punch 1

punch 4

Fig. 6. View of distorted punches.

TABLE 2

Set prescribed displacements of the nodes at the top surface of the punch

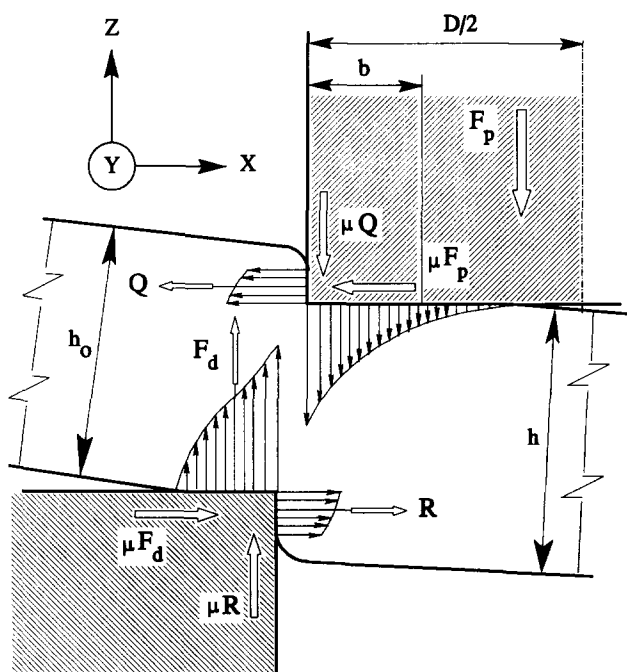| Node No.	Prescribed displacement (mm)		
	u	v	w
232	0.0	0.0	0.0
281	0.0	0.0	0.0
285	0.0	0.0	0.0
289	0.0	0.0	0.0
293	0.0	0.0	0.0

Fig. 7. Load on the cutting edge of the punch.

$$F_p = \tfrac{1}{3}\pi\sqrt{3}\, D\, h\, C\, [k \ln (h_0/h)]^n \qquad (3)$$

and hence the maximum force by

$$F_{pmax} = \tfrac{1}{3}\pi\sqrt{3}\, D\, h_0\, C\, [n/e]^n\, k^n \qquad (4)$$

when neglecting the influence of friction.

From the theory of plastic instability it is shown easily that the tensile strength of a material can be expressed in terms of:

$$\sigma_B = C \, [n/e]^n \tag{5}$$

or

$$\sigma_B = C \, e^{\bar{\epsilon}_0} \, [n/e]^n \tag{6}$$

in the case where initial deformation $\bar{\epsilon}_0$ is present. Substitution of the expression for σ_{B_0} (eqn. (5)) in eqn. (4) renders:

$$F_{pmax} = \pi \, D \, h_0 \, k_f \, \sigma_{B_0} \tag{7}$$

where $k_f = \frac{1}{3} \, k^n \sqrt{3}$ represents the shear factor in punching. The parameter k is approximately a constant, characteristic for the process describing the relationship between the geometrical measure of deformation h_0/h and some average of the effective deformation physically present in the entire shearing zone. The parameters h_0 and h are the initial and instantaneous blank thicknesses, respectively, C is the stress characteristic, n is the strain-hardening exponent, σ_{B_0} is the ultimate tensile strength of the blank material and D is the diameter of the punch.

Referring to Fig. 7, the radial component friction forces F_x $(= -\mu F_p)$, F_y $(= \mu F_p)$ and thrust component F_z $(= F_p)$ per unit length in terms of punching force F_p can be determined as:

$$\begin{bmatrix} F_x \\ F_y \\ F_z \end{bmatrix} = \mu \begin{bmatrix} \sin\theta & 0 & 0 \\ 0 & \cos\theta & 0 \\ 0 & 0 & 1/\mu \end{bmatrix} \begin{bmatrix} F_p \\ F_p \\ F_p \end{bmatrix} \tag{8}$$

where θ is in degrees and defines the position of a nodal load on the punch circumference in the XY-plane (Figs. 2 or 8).

Since the punch point shear angle is ϕ (Fig. 9), the radial component force F_x and axial or thrust component F_z and the normal force $(F_n = F_p)$ per unit length that are applicable to punches 2 and 3 are

$$\begin{bmatrix} F_x \\ F_y \\ F_z \end{bmatrix} = \begin{bmatrix} \sin\phi & 0 & 0 \\ 0 & \sin\phi & 0 \\ 0 & 0 & \cos\phi \end{bmatrix} \begin{bmatrix} F_p \\ F_p \\ F_p \end{bmatrix} \tag{9}$$

whilst for the case applicable to punch 4 these forces are as follows:

$$\begin{bmatrix} F_x \\ F_y \\ F_z \end{bmatrix} = \begin{bmatrix} \sin\phi & 0 & 0 \\ 0 & \mu\sin\phi & 0 \\ 0 & 0 & \cos\phi \end{bmatrix} \begin{bmatrix} F_p \\ F_p \\ F_p \end{bmatrix} \tag{10}$$

The distribution of the normal pressure to the three node points on the cutting edge is now considered. If F_p is a load distributed from r to R as shown in Fig.
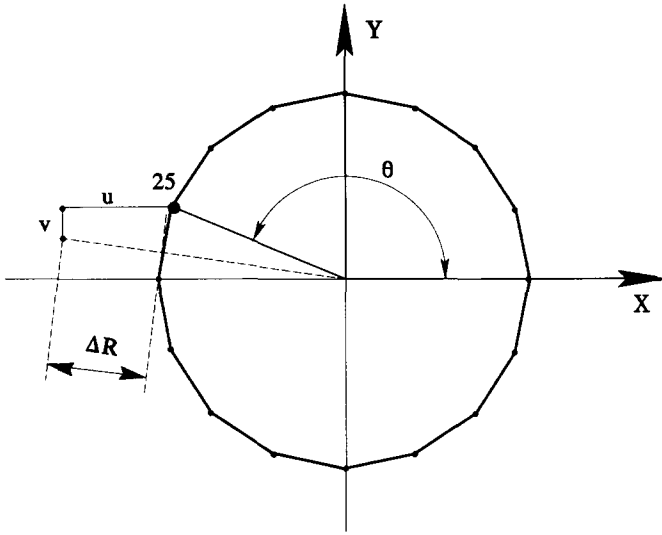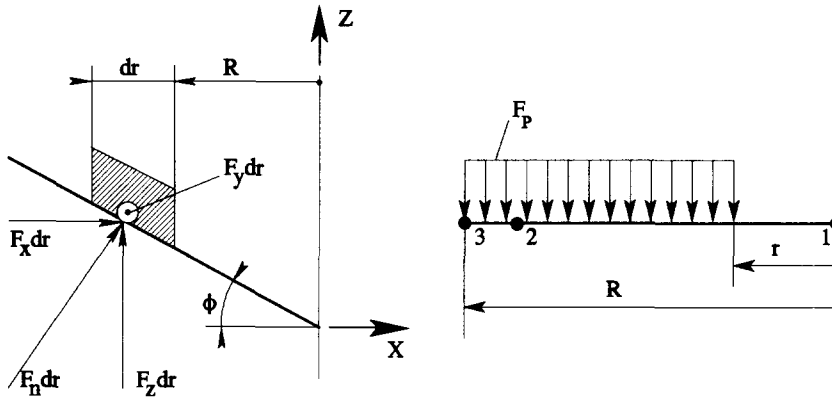
Fig. 8. Radial deformation.

Fig. 9. Load on the cutting edge of a punch of shear angle φ.

Fig. 10. Distribution of load.

10, the three nodal loads in the direction of F_p for an 8-node element are given by:

$$
\begin{bmatrix} F_{p1} \\ F_{p2} \\ F_{p3} \end{bmatrix} = F_p R \begin{bmatrix} \frac{1}{12} & -\frac{1}{2} & \frac{3}{4} & -\frac{1}{4} \\ \frac{1}{6} & 0 & -\frac{1}{2} & \frac{1}{4} \\ \frac{1}{12} & 0 & \frac{1}{4} & -\frac{1}{4} \end{bmatrix} \begin{bmatrix} 1 \\ \zeta \\ \zeta^2 \\ \zeta^3 \end{bmatrix}
\tag{11}
$$

where $\zeta = r/R$. Loads F_x, F_y and F_z have to be distributed to the nodes on the cutting edge according to eqn. (11).

TABLE 3

Nodal loads on the cutting edge surface

Punch profile No.	Shear angle ϕ (degrees)	Node No.	Force (N)		
			F_x	F_y	F_z
1, 5, 6	0	1	248	−248	2482
		10	1003	−1003	10027
		26	3266	−3266	32656
2, 3	22.5	1	948	−948	2293
		10	3837	−3837	9264
		26	12497	−12497	30170
4	22.5	1	12497	−1250	30170
		10	3837	−384	9264
		26	948	−95	2293

For numerical computations, the following punch and blank geometry is used: punch diameter $D = 12$ mm; blank thickness $h_0 = 6$ mm; ultimate tensile strength of the blank material $\sigma_{B_0} = 520$ N/mm^2; $k = 2.92$ (after eqn. (7)); strain-hardening exponent $n = 0.264$; $b = R - r = (2\text{-}3.5)\delta$ as in Ref. [8]; the clearance between die and punch $\delta = 0.1 h_0$; and the coefficient of friction $\mu = 0.10$.

For the steel, Young's modulus is 210 GPa and Poisson's ratio is 0.3; whilst for the hard metal these quantities are 500 GPa and 0.22, respectively.

Substitution of the pressure distribution given by eqn. (11) into eqns. (8)–(10) results in the nodal forces at 1, 10, and 26 (Fig. 2) for $\xi = 0.666$, as shown in Table 3. The model of each of the punches 1, 2, 3, 5 and 6 consists of 184 linear hexadredronal elements whilst the model of punch 4 is composed of 183 linear hexahedral elements.

3. Punch deformation

The nodal-point deformations of the punch are represented by u, v and w which are the x, y and z component displacements, respectively. The displacement of the outermost node, for example node number 25, of the punch is of interest as this is related directly to the performance of the tool, the radial displacement ΔR representing the variation in punch size and position whilst cutting. Referring to Fig. 8, ΔR is given precisely by

$$\Delta R = [(R \cos \theta + u)^2 + (R \sin \theta - v)^2]^{1/2} - R \qquad (12)$$

4. Results

Before carrying out an investigation into the design parameters of a punch,

an assessment of the reliability of the finite-element model is needed. For the FE model to be valid, the model results have to be compared to either experimental results or to experimental data established by others. In this case the FE force model which has a direct relationship with the tool deformation, is compared to and checked against the experimental force data produced by the American Society of Manufacturing Engineers (SME) [7] and by Ramanovsky [8].

4.1. Evaluation with respect to punch load

In Fig. 11, results are shown for the punch load as a function of the shear angle, ϕ, from which it is seen that punch load F_z reduces gradually as the shear angle (or the shear height) increases, whilst punch loads F_x and F_y rises sharply with increasing shear angle. Comparison of results between the FE force model and SME displays a fair correlation and thus establishes the validity of the finite-element model. The results also highlight that the effect of punch loads F_x or F_y or a combination of both could be severe on the performance of a tool if a punch with one-way shear, for example punch 4, is used (Fig. 12).

4.2. Tool design considerations

From the point of view of machine-tool users, tooling aspects of production such as tool failure and deterioration in the dimensional accuracy of a manufactured component, are particularly important. The performance of a tool will be considerably enhanced if a punch of particular design (Fig. 1) is employed. Consequently, the design parameters of a punch such as the shear relief angle
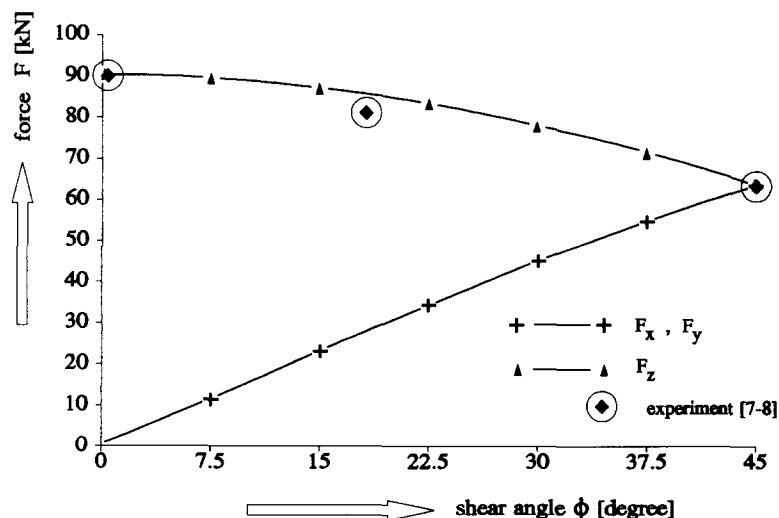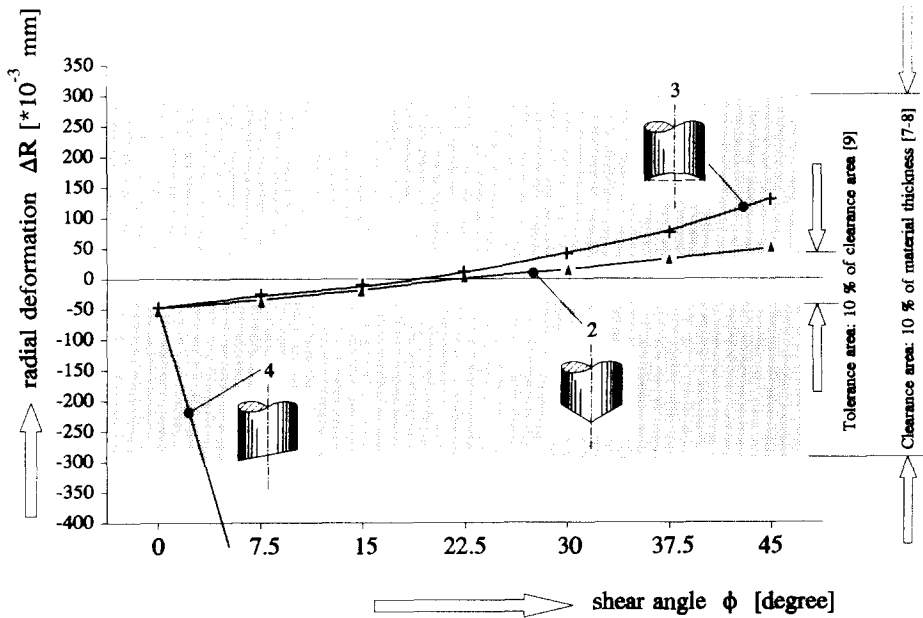
Fig. 11. Punch load versus shear angle φ.

Fig. 12. Radial deflection versus shear angle φ.

on the face of the punch, the shape of the cutting profile and tool material characteristics, are of interest.

Figure 13 shows the radial stiffness of various types of tools. The shear angle, ϕ, for punches 2, 3 and 4 is 22.5° whilst for punches 1, 5 and 6, $\phi = 0$°. Comparison of the results shows the measure of improvement in tool performance if punch 2, with balanced convex shear, is employed. The results suggest that the use of punch 2 is most desirable if high dimensional accuracy of a component is required, and a thicker or more resistant blank material is to be punched on the same press.

Figure 14 depicts the axial stiffness of various types of punches for the shear angles as given above, comparison of the results demonstrating the superiority of punch 6 over all other types of punches. The results suggest that the use of punch 6, with sintered hard metal around its circumferential cutting edge, may be quite desirable if the punch encounters no eccentric load (see Fig. 13).

The relationship for the radial deflection, ΔR, of punches 2, 3 and 4 as a function of shear angle, ϕ, is illustrated in Fig. 12. Analysis of the results reveals that a shear angle of between 17°–22° results in a minimum radial deformation for the punches 2 and 3, which implies that punches 2 and 3 with shear angle $\phi \simeq 20$° can be employed in practice safely in order to satisfy the tolerance criterion [7–9] for manufactured components made of a range of materials such as aluminium alloys, brass, cold-rolled steel and stainless steel. The radial deflection of punch 4 deteriorates with increasing shear angle. The
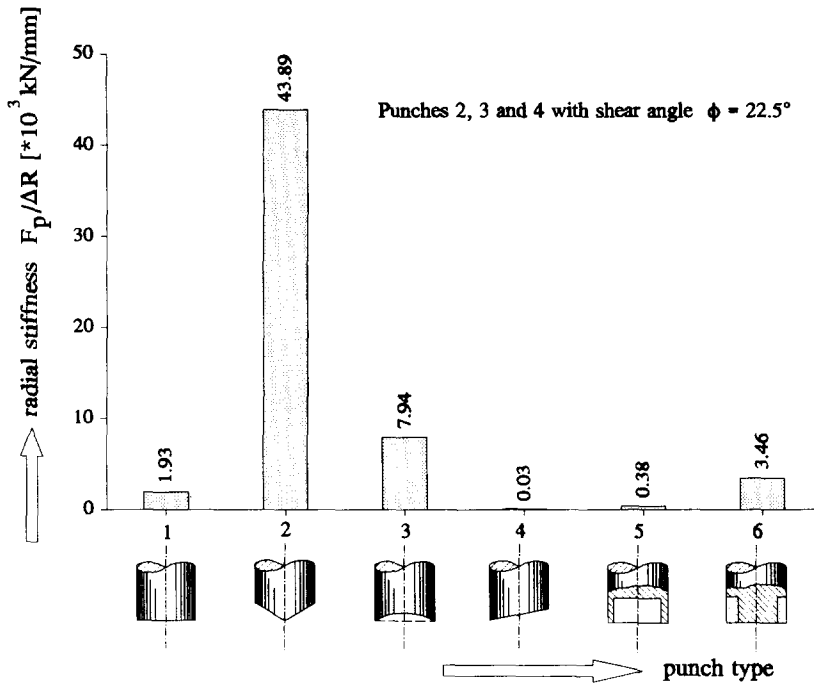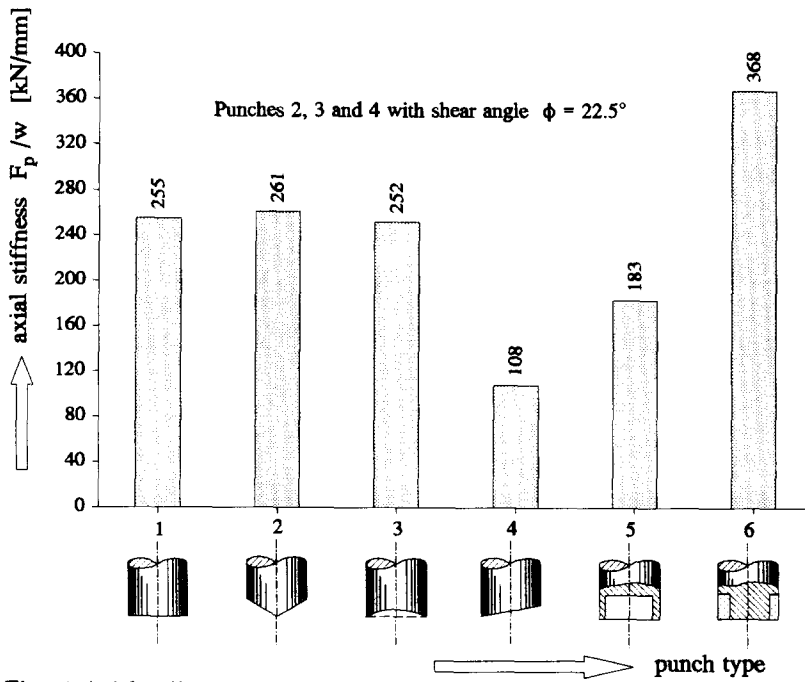
Fig. 13. Radial stiffness versus punch type.

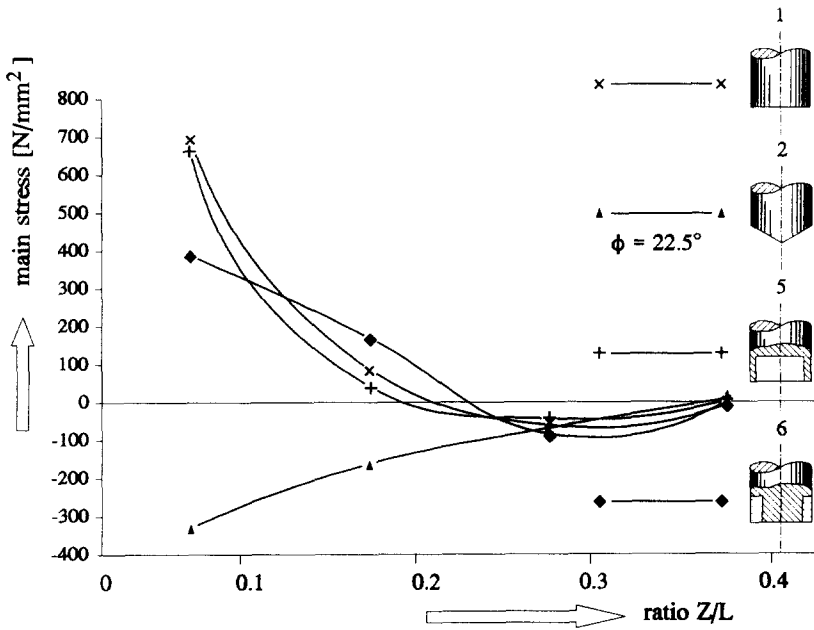Fig. 14. Axial stiffness versus punch type.

Fig. 15. Main principal stress versus ratio Z/L.

results also suggest that a shear angle above $2°-3°$ for punch 4, with one-way shear, is undesirable as this may cause the dimensional accuracy of a component to be impaired. This clearly underlines the importance of punch design, both for tool life and in securing the dimensional accuracy of the components to be manufactured.

Figure 15 shows the main principal stress for punches 1, 2, 5 and 6 as a function of dimensionless parameter Z/L of the punch, where Z is a variable position of a point on the circumferential surface along the axial length of the punch and L is the total length of the punch. The results indicate that the stress is at its maximum near to the cutting edge of the punch and tends to fall sharply as the ratio Z/L increases. Comparison of the results shows the degree of improvement in reduction of stress on the tool if punch 2, with balanced shear, is used.

5. Conclusions

(1) The present study on punch design has resulted in the development of 3-D finite-element models of various types of punches (Fig. 1) and demonstrates the usefulness of these models in solving practical problems involving a range of design parameters.

(2) That the radial deformations of punches with balanced convex and con-

cave shear have a minimum value within the shear angle range of 17°–22° suggests that a shear angle of 20° can be proposed safely for practical purposes.

(3) That amongst the rigidity characteristics evaluated for all types of punches, the punch with balanced convex shear, 2, shows the best performance (Figs. 13 and 15), suggests that this type of punch can reasonably be recommended in practice in order to reduce the stress on the tool and thus to enable thicker or more resistant stock to be punched on the same press or to permit the use of a lower-rated press.

(4) Since the inclusion of eccentricity due to assymmetric load on the press is an important factor in the punching/blanking process [6], the choice of punch 2, with balanced convex shear, against punch 6, with sintered hard metal around its circumferential cutting edge, is obvious (Fig. 11), despite the axial stiffness of punch 6 having a substantially greater competitive edge than punch 2.

Acknowledgements

References

1   U.P. Singh, P.C. Veenstra and J.A. Ramaekers, Numerical analysis of the distortional behaviour of a hydraulic press, *Ann. CIRP,* 16(1) (1977) 119.
2   U.P. Singh, Design analysis of a single column pressframe, *ASME Trans., J. Vibr. Acoust. Stress Reliab.,* 106 (October 1984) 508–516.
3   U.P. Singh, R. Wilson and S. Hinduja, Computer aided study of a single column hydraulic press, *Proc. 25th Int. Machine Tool Design and Research Conf.,* Birmingham, April, 1985, Macmillan, London, pp. 389–395.
4   J.A. Hijink and A.C.H. vander Wolf, On the design of die-sets, *Ann. CIRP,* 24 (1975) 127.
5   U.P. Singh and P.P. Miller, Computer aided design of a die-set, *Proc. 2nd Conf. of the Irish Manufacturing Committee,* Jordanstown, September, 1985, pp. 637–651.
6   U.P. Singh, H.J.J. Kals and A.H. Streppel, Computer aided design study of a die-set for punching/blanking, *Proc. 28th Int. Machine Tool Design and Research Conf.,* Manchester, April, 1990, Macmillan, London, pp. 379–386.
7   Tools and Manufacturing Engineers Handbook, 3rd edn., McGraw-Hill, New York, 1976, pp. 4.5–4.12.
8   N.P. Ramanovsky, *Hand Book on Die Design,* 5th edn., Mashinostroenia, Leningrad, 1971, pp. 26–30.
9   Donald F. Early, Press alignment, *Tool Manuf. Eng.,* 42(6) (1962).